

# Structural Chemistry of the Neptunium–Germanium Binary System

P. Boulet,<sup>1</sup> D. Bouëxière, J. Rebizant, and F. Wastin

European Commission, Joint Research Centre, Institute for Transuranium Elements, Postfach 2340, 76125 Karlsruhe, Germany

Received June 26, 2000; in revised form September 20, 2000; accepted October 6, 2000; published online December 21, 2000

The structural chemistry of the complete binary neptunium–germanide system has been investigated by means of X-ray diffraction. In addition to the well-known  $\text{NpGe}_3$  (AuCu<sub>3</sub> type), at least five new binary phases have been found. The crystal structure of  $\text{NpGe}_{2-x}$  (defect ThSi<sub>2</sub> type),  $\text{NpGe}_{2-x}$  (defect AlB<sub>2</sub> type),  $\text{NpGe}$  (USi type),  $\text{Np}_5\text{Ge}_4$  (Ti<sub>5</sub>Ga<sub>4</sub> type), and  $\text{Np}_5\text{Ge}_3$  (W<sub>5</sub>Si<sub>3</sub> type) have been refined from single-crystal and powder X-ray diffraction data. X-ray powder analyses by Rietveld-type profile refinement revealed a small homogeneity range of the three first phases, as usually observed with the rare-earth or uranium isotopic compounds, whereas  $\text{Np}_5\text{Ge}_4$  and  $\text{Np}_5\text{Ge}_3$  seem to be line compounds as the unit cell parameters were independent of the starting composition. The formation and the homogeneity range of these new phases are discussed, and the structural evolution is compared with the analogous uranium binary system. © 2001 Academic Press

**Key Words:** crystal structure; neptunium; intermetallic compounds.

## INTRODUCTION

Intermetallic compounds  $R-T-X$ , where  $R$  is either a rare-earth or an actinide,  $T$  is a transition metal, and  $X$  is a metalloid element, have been intensively studied during the past 20 years. Many new compounds with different compositions and crystallizing with distinct structure types have been discovered. Particular interest has been devoted to special ternary families of compositions such as 1-2-2(1), 2-2-1(2,3), or 2-3-4(4-5). As a result of the intensive experimental and theoretical investigations, it was established that their electronic properties are mainly governed by the strength of the  $f$  ( $spd$ ) hybridization, i.e., the interaction of the  $f$  electrons with the conduction electrons. However, many conflicting results were reported on the same compounds due to the fact that these physical properties are very sensitive to elements of the “history” of the sample like heat treatment, homogeneity, or impurities. To know the intrinsic physical properties of these compounds, the first

step is to determine the relation of equilibrium with the neighboring phases and to evaluate their homogeneity range. As a contribution to this subject the correct determination of the binary phase diagram itself is a prerequisite, and recently, binary uranium phase diagrams, like those of U–Si (6), U–Ge(7–10), and U–Sn(11), were reported, showing interesting properties ranging from paramagnetism to long-range magnetic order and/or superconductivity. Taking into account these new results, a literature search shows that the corresponding binary phase diagram with actinide elements like neptunium and plutonium were not well characterized. Therefore, within our program on strongly correlated  $5f$  electron systems, the complete Np–Ge binary system has been investigated and we present the results of our X-ray analysis.

## EXPERIMENTAL

Polycrystalline ingots were obtained by arc melting stoichiometric amounts of the constituent elements under an atmosphere of high-purity argon on a water-cooled copper hearth, using a Zr alloy as an oxygen getter. The materials were used in the form of ingots as supplied by Merck AG (germanium 4 N pure) and by LANL (neptunium 3 N pure). In order to ensure homogeneity, the arc-melted buttons were turned over and remelted three times, with weight losses lower than 0.5%. The samples were checked by X-ray powder diffraction data ( $\text{CuK}\alpha_{1,2}$  radiation) collected on a Bragg–Brentano Siemens D500/501 diffractometer using a  $2\theta$  step size of  $0.02^\circ$ . The diffraction patterns were analyzed by a Rietveld-type profile refinement method using the Fullprof program (12). The single-crystal X-ray diffraction data were collected on a Enraf-Nonius CAD-4 four-circle diffractometer using a monochromated  $\text{MoK}\alpha$  wavelength. The data processing was carried out using the Molen package (13).

## X-RAY STRUCTURAL CHARACTERIZATION

### $\text{NpGe}_3$

The binary richest in germanium,  $\text{NpGe}_3$ , is the only phase that has already been reported in this system (14). It

<sup>1</sup> To whom correspondence should be addressed. Fax: 00(49) 07247 951 593. E-mail: Boulet@itu.fzk.de.

crystallizes with the cubic AuCu<sub>3</sub> type, and the lattice parameter obtained by full-profile refinement on D500 powder data ( $a = 4.2114(9) \text{ \AA}$ ) is in good agreement with the values usually reported in the literature ( $a = 4.213$ ). Magnetic investigations (15) of this phase show that it does not order magnetically down to 1.7 K. Particular interest has been devoted to this family of compounds since it belongs to the series  $AnX_3$  with  $An =$  actinide and  $X =$  Al, Ga, In, Pb, Si, Ge, and Sn. All of these compounds have  $An$ - $An$  interatomic distances larger than the Hill limit and exhibit different magnetic properties, going from independent paramagnetism to ferro/antiferromagnetic, emphasizing the dominant role of the  $5f$ - $spd$  (ligands) hybridization in the localization/delocalization process.

### $NpGe_{2-x}$

The defect disilicide or digermanide compounds with rare earth or actinide elements are known to crystallize in two types of structures, a tetragonal ThSi<sub>2</sub> type and a hexagonal AlB<sub>2</sub> type. As usually observed in these systems, both struc-

tural modifications were encountered in the Np-Ge binary system.

The X-ray powder analyses of the as-cast sample with nominal composition Np<sub>3</sub>Ge<sub>5</sub>, i.e., NpGe<sub>2-x</sub>,  $x = 0.34$ , was indexed with a body-centered tetragonal unit cell with  $a = 4.0867(2) \text{ \AA}$  and  $c = 13.921(1) \text{ \AA}$ , revealing a single-phase product for this composition. Single crystals suitable for crystal structure determination were easily extracted from this sample, showing in particular that this phase crystallizes either congruently or by a peritectic transformation. The single-crystal X-ray diffraction data were collected on an Enraf-Nonius CAD-4 four-circle diffractometer with the experimental conditions listed in Table 1. The X-ray diffraction intensities were corrected for Lorentz and polarization effects, and an absorption correction was applied using the psi-scan method. The structure was successfully refined in the centrosymmetric space group  $I4_1/amd$  with the reliability factors  $R = 0.062$ ,  $R_w = 0.086$ . NpGe<sub>2-x</sub> crystallizes with the ThSi<sub>2</sub> structure type with, as expected, a deficient occupancy factor for the germanium crystallographic site, leading to the composition NpGe<sub>1.72(4)</sub> for the

**TABLE 1**  
**X-Ray Crystallographic Data for NpGe<sub>2-x</sub> (ThSi<sub>2</sub> Type), Atomic Parameters, and Interatomic Distances**

Method	single-crystal refinement								
Space group	$I4_1/amd$ , no. 141, origin at $-1$								
Linear absorption coefficient ( $\text{cm}^{-1}$ )	793.0								
Lattice parameters (from CAD4)( $\text{\AA}$ )	$a = 4.080(1) \text{ \AA}$ , $c = 13.909(3) \text{ \AA}$ , $V = 231.6(2) \text{ \AA}^3$ , $d_{\text{calc}} = 10.99 \text{ gcm}^{-3}$ , $Z = 4$ , $M = 354.6 \text{ g}$								
Scan range	$2 < \theta < 30$ $-5 < h < 5$ , $-5 < k < 5$ , $-19 < l < 19$								
Total observed reflections	1510								
Total observed reflections after average	257								
Independent reflections with $I > 3\sigma$	93								
Secondary extinction coefficient	$g = 1.038 \times 10^{-6}$ , corr. = $1/(1 + gIc)$								
Number of variables	9								
Reliability factors:	0.062								
$R = \sum [ F_o  -  F_c ] / \sum  F_o $	0.086								
$R_w = [\sum_w ( F_o  -  F_c )^2 / \sum_w  F_o ^2]^{1/2}$									
Goodness of fit, GOF	3.16								
Atom parameters									
Atom	Site	$x$	$y$	$z$	$B(1,1)$	$B(2,2)$	$B(3,3)$	$B$ in $\text{\AA}^2$	$\tau_{\text{occ}}$
Np	4a	0	$\frac{3}{4}$	1/8	0.56(6)	$B(1, 1)$	0.63(8)	0.61(3)	1
Ge	8e	0	$\frac{1}{4}$	0.2927(8)	5.0(7)	0.5(3)	4.4(4)	3.3(2)	1.72(4)
Interatomic distances (in $\text{\AA}$ )									
Central atom: Np					Central atom: Ge				
Ligand atom		Distance			Ligand atom		Distance		
4Ge		3.099(9)			1Ge		2.29(2)		
8Ge		3.104(4)			2Ge		2.361(8)		
4Np		4.031(0)			2Np		3.099(9)		
4Np		4.080(0)			4Np		3.104(4)		

Note. The form of the anisotropic displacement parameter is  $\exp \left[ -\frac{1}{4} (h^2 a^{*2} B(1, 1) + k^2 b^{*2} B(2, 2) + l^2 c^{*2} B(3, 3) + 2hka^* b^* B(1, 2) + 2hla^* c^* B(1, 3) + 2klb^* c^* B(2, 3)) \right]$ , where  $a^*$ ,  $b^*$ , and  $c^*$  are reciprocal lattice constants.

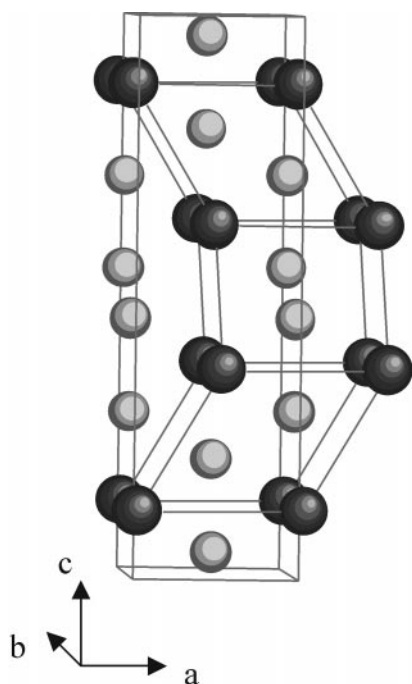


FIG. 1. View of  $\text{NpGe}_{2-x}$  ( $\text{ThSi}_2$  type) crystal structures; the distorted  $\text{AlB}_2$  blocks are shown.

crystal studied. The positional and thermal parameters and the main interatomic distances are listed in Table 1. A view of the structure is illustrated in Fig. 1 with, as for the other structure figures, the neptunium atoms in black and the germanium atoms in light gray.

The X-ray powder patterns of samples with nominal composition  $\text{Np}_3\text{Ge}_{4.8}$  were indexed on the basis of a hexagonal unit cell with  $a = 3.9686(2) \text{ \AA}$  and  $c = 4.1705(3) \text{ \AA}$ . Single crystals suitable for crystal structure determination were easily obtained from the as-cast samples. As shown in Table 2, the structure was successfully refined in the space group  $P6/mmm$  (no. 191) with the reliability factors  $R = 0.085$ ,  $R_w = 0.095$ . This phase crystallizes with the  $\text{AlB}_2$  structure type with, as expected, a deficient occupancy factor for the germanium site, leading to the composition  $\text{NpGe}_{1.59(4)}$  for the crystal studied. The positional and thermal parameters and the main interatomic distances are listed in Table 2. A view of the crystal structure is illustrated in Fig. 2. Besides this, it has to be mentioned that as usually observed with the  $M_3T_5$  binary compounds, where  $M$  is a rare earth or actinide elements and  $T$  is a metalloid element like Si or Ge, indication of a supercell structure has been evidenced from the X-ray powder as well as the single-crystal data. It is worth mentioning here that the  $\text{AlB}_2$  type is rarely encountered without these superstructure lines (10), which are due to the ordering of the germanium vacancies, but no real successful crystal structure determination had been reported yet for this type of structure. The  $\text{ThSi}_2$  type

TABLE 2  
X-Ray Crystallographic Data for  $\text{NpGe}_{2-x}$  ( $\text{AlB}_2$  Type),  
Atomic Parameters, and Interatomic Distances

Method	single-crystal refinement
Space group	$P6/mmm$ , no. 191
Linear absorption coefficient ( $\text{cm}^{-1}$ )	804.9
Lattice parameters (from CAD4)( $\text{Å}$ )	$a = 3.9686(2) \text{ \AA}$ , $c = 4.1705(3) \text{ \AA}$ , $V = 56.958(5) \text{ \AA}^3$ , $d_{\text{calc}} = 10.42 \text{ g cm}^{-3}$ , $Z = 1$ , $M = 357.5 \text{ g}$
Scan range	$2 < \theta < 30$ , $-7 < h, k, l < 7$
Total observed reflections	1412
Independent reflections with $I > 3\sigma$	99
Secondary extinction coefficient	$g = 3.045 \times 10^{-6}$ , corr. = $1/(1 + gIc)$
Number of variables	7
Reliability factors:	0.085
$R = \sum[ F_o  -  F_c ]/\sum F_o $	0.095
$R_w = [\sum_w( F_o  -  F_c )^2/\sum_w F_o ^2]^{1/2}$	
Goodness of fit, GOF	2.59

Atom	Site	Atom parameters						
		$x$	$y$	$z$	$B(1, 1)$	$B(3, 3)$	$B$ in $\text{Å}^2$	$\tau_{\text{occ}}$
Np	1a	0.0	0.0	0.0	0.87(5)	0.33(5)	0.69(2)	1
Ge	2d	1/3	2/3	1/2	5.8(4)	0.6(2)	4.0(2)	1.59(4)

Interatomic distance (in $\text{Å}$ )			
Central atom: Np		Central atom: Ge	
Ligand atom	Distance	Ligand Atom	Distance
12Ge	3.098(1)	3Ge	2.291(1)
6Np	3.968(1)	6Np	3.098(1)

Note. The form of the anisotropic displacement parameter is  $\exp[-\frac{1}{4}(h^2a^*{}^2B(1, 1) + k^2b^*{}^2B(2, 2) + l^2c^*{}^2B(3, 3) + 2hka^*b^*B(1, 2) + 2hla^*c^*B(1, 3) + 2klb^*c^*B(2, 3))]$ , where  $a^*$ ,  $b^*$ , and  $c^*$  are reciprocal lattice constants;  $B(1, 2) = B(2, 2) = B(1, 1)$ ,  $B(1, 3) = B(2, 3) = 0.0$ .

and  $\text{AlB}_2$  type are quite correlated and could be derived one from the other. The  $\text{ThSi}_2$  type is built up from distorted  $\text{AlB}_2$  blocks which are alternatively translated by  $\frac{1}{2}a$  and  $\frac{1}{2}b$  along the  $c$  axis. As mentioned by Venturini *et al.* (16), the transformation of the tetragonal  $\text{ThSi}_2$  type into the

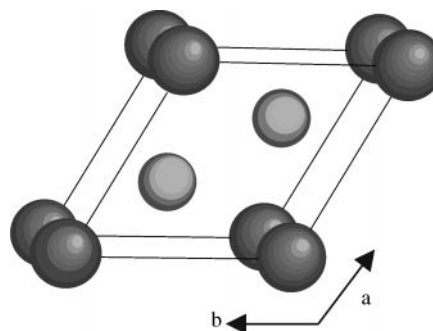


FIG. 2. View of  $\text{NpGe}_{2-x}$  ( $\text{AlB}_2$  type) crystal structure.

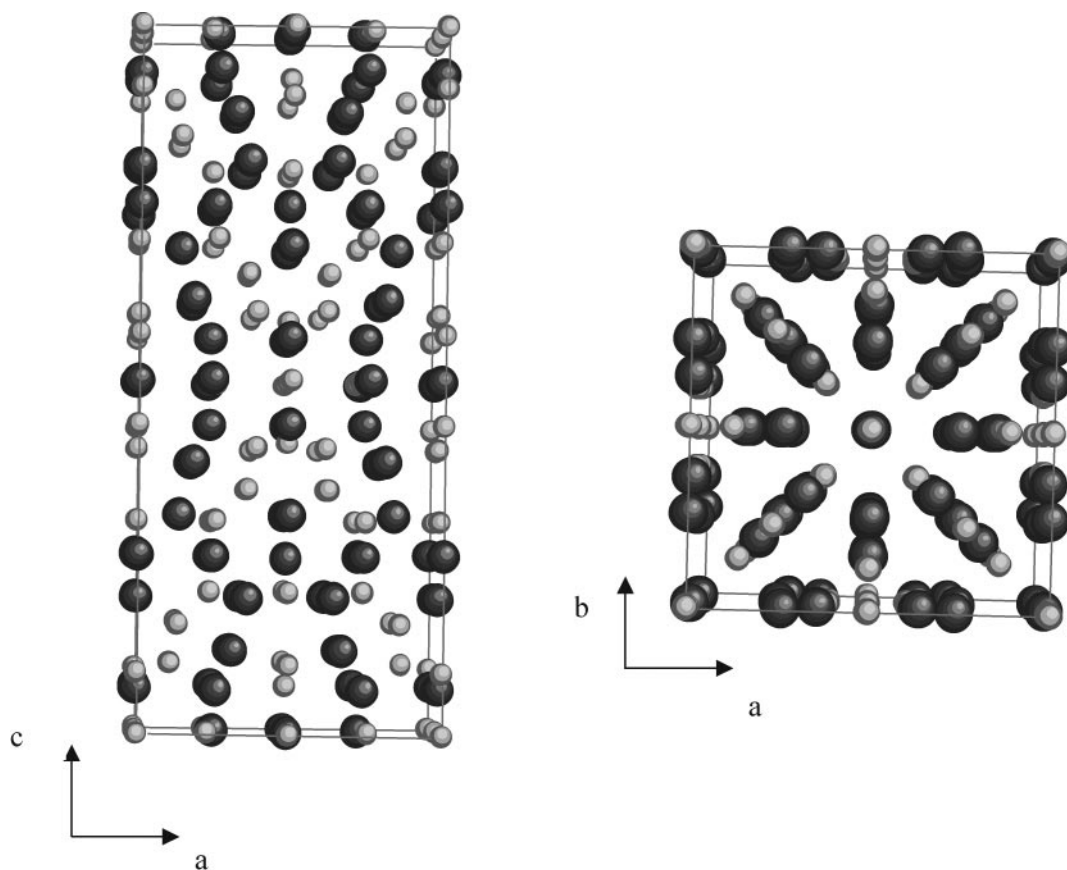


FIG. 3. View of the NpGe (USi type) crystal structure.

hexagonal  $AIB_2$  type is not simple and goes through many different supercells, depending on the exact content on germanium vacancies.

Finally, it was found that this phase exhibits a slight homogeneity range. From the starting composition  $Np_3Ge_4$ , a two-phase Rietveld refinement of the powder

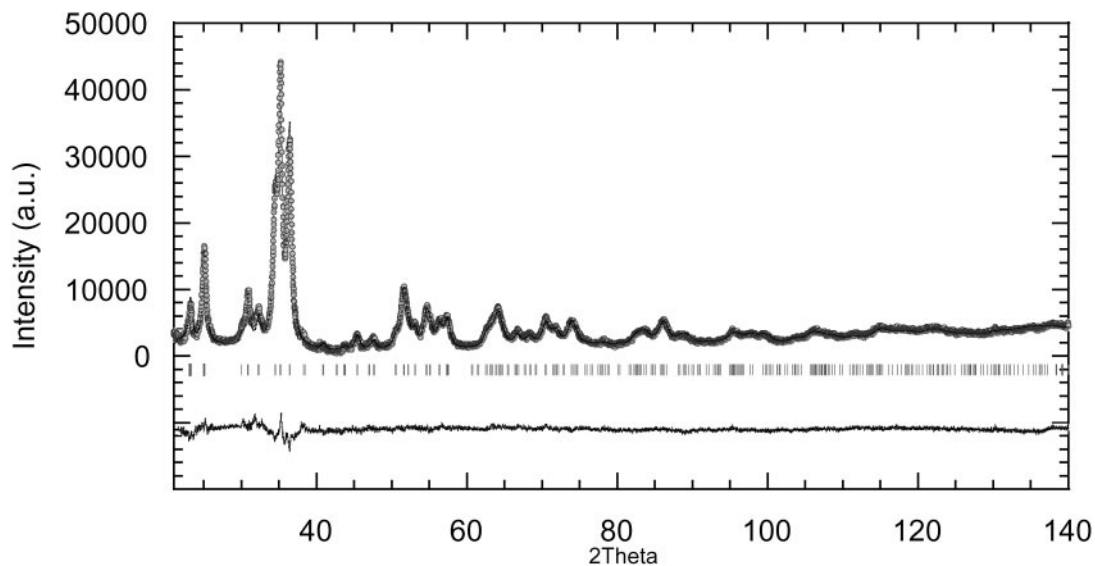


FIG. 4. X-ray powder diffraction pattern of  $Np_5Ge_4$  ( $Ti_5Ga_4$  type). The symbols represent the observed points; the solid lines represent the calculated profile and the difference between observed and calculated profiles. The ticks correspond to  $2\theta_{hkl}$  Bragg positions.

**TABLE 3**  
X-Ray Crystallographic Data for NpGe (USi Type) and Atomic Parameters

Method	single-crystal refinement
Space group	$I4/mmm$ , no. 139, origin at $-1$
Linear absorption coefficient ( $\text{cm}^{-1}$ )	1052.2
Lattice parameters (from CAD4)(Å)	$a = 10.9117(6)$ Å, $c = 25.358(1)$ Å, $V = 3019.3(4)$ Å <sup>3</sup> , $d_{\text{calc}} = 11.01$ gcm <sup>-3</sup> , $Z = 68$ , $M = 309.6$ g
Scan range	$2 < \theta < 30$ $-16 < h < 16$ , $-16 < k < 0$ , $-36 < l < 0$
Total observed reflections	4672
Total observed reflections after average	1309
Independent reflections with $I > 3\sigma$	803
Secondary extinction coefficient	$g = 2.5992 \times 10^{-8}$ , corr. = $1/(1 + gIc)$
Number of variables	34
Reliability factors: $R = \sum [ F_o  -  F_c ] / \sum  F_o $ $R_w = [\sum_w ( F_o  -  F_c )^2 / \sum_w  F_o ^2]^{1/2}$	0.071 0.092
Goodness of fit, GOF	2.72

Atom	Site	Atom parameters			$B$ in Å <sup>2</sup>	$\tau_{\text{occ}}$
		$x$	$y$	$z$		
Np(1)	4e	0.0	0.0	0.2528(2)	0.91(8)	1
Np(2)	8f	$\frac{1}{4}$	$\frac{1}{4}$	$\frac{1}{4}$	0.69(5)	1
Np(3)	8j	0.2623(4)	$\frac{1}{2}$	0.0	0.56(5)	1
Np(4)	16n	0.0	0.2579(3)	0.0617(1)	0.64(4)	1
Np(5)	16n	0.0	0.3584(3)	0.1907(1)	0.98(4)	1
Np(6)	16m	0.1832(2)	—	0.3840(1)	0.67(4)	1
Ge(1)	2a	0.0	0.0	0.0	2.5(6)	1
Ge(2)	4c	0.0	$\frac{1}{2}$	0.0	0.2(2)	1
Ge(3)	4e	0.0	0.0	0.095(2)	0.3(6)	0.38(1)
Ge(4)	4e	0.0	0.0	0.4309(6)	0.3(2)	1
Ge(5)	8h	0.2368(7)	—	0.0	0.3(1)	1
Ge(6)	16n	0.0	0.2574(7)	0.2996(3)	0.4(1)	1
Ge(7)	16n	0.0	0.3791(7)	0.3990(3)	0.4(1)	1
Ge(8)	16m	0.1352(5)	—	0.1551(3)	0.6(1)	1

diffraction data, showing the equilibrium between the  $\text{AlB}_2$  type and the neighboring binary phase NpGe (see below), leads to the lattice parameters  $a = 3.9712(2)$  Å,  $c = 4.1702(2)$  Å and to an occupation factor of 1.48(1) Ge, i.e., approximately  $\text{Np}_2\text{Ge}_3$ .

### NpGe

Increasing the content of neptunium in our samples shows that the next binary phase in the Np–Ge binary system melts congruently since single crystals could be easily obtained from the as-cast samples. The single-crystal

X-ray diffraction data were collected with the experimental conditions listed in Table 3. The tetragonal lattice constants, determined from least-squares analysis of the setting angles of 25 X-ray reflections have the values  $a = 10.889(3)$  Å and  $c = 25.327(8)$  Å. The X-ray diffraction intensities were corrected for Lorentz and polarization effects, and an absorption correction was applied using the psi-scan method. The inspection of the systematic extinctions revealed that  $hkl$ ,  $h + k + l = 2n$  were not present. The structure was successfully refined in the body-centered space group  $I4/mmm$  with the reliability factors  $R = 0.088$ ,  $R_w = 0.111$  using the atomic position reported for USi (17). The correct formula obtained is thus  $\text{Np}_{68}\text{Ge}_{70}$ ; however, as also observed for USi, large isotropic factors of some Ge sites, namely, Ge(1)

**TABLE 4**  
X-Ray Crystallographic Data for  $\text{Np}_5\text{Ge}_4$  ( $\text{Ti}_5\text{Ga}_4$  Type), Atomic Parameters, and Interatomic Distances

Method	full profile refinement of X-ray powder diffraction data
Space group	$P6_3/mcm$ , no. 193
Lattice parameters (Å)	$a = 8.8004(9)$ Å, $c = 5.9274(7)$ Å, $V = 397.56(7)$ Å <sup>3</sup> , $Z = 2$ , $M = 1475.6$ g
Scan range	$20 < 2\theta < 140$
Number of reflections used in refinement	313
$R_B$	0.071
$R_f$	0.041
$R_p$	0.108
$R_{wp}$	0.138

Atom	Site	Atom parameters			$B$ in Å <sup>2</sup>	$\tau_{\text{occ}}$
		$x$	$y$	$z$		
Np	4d	$\frac{1}{3}$	$\frac{2}{3}$	0	0.57(1)	1
Np	6g	0.2761(1)	0.0	$\frac{1}{4}$	0.57(1)	1
Ge	6g	0.6192(4)	0.0	$\frac{1}{4}$	0.78(2)	1
Ge	2b	0.0	0.0	0.0	0.37(2)	1

Interatomic distances (in Å)			
Central atom: Np(1)		Central atom: Np(2)	
Ligand atom	Distance	Ligand atom	Distance
2Np(1)	2.963(0)	2Ge(2)	2.848(1)
6Ge(1)	3.136(1)	2Ge(1)	2.966(2)
6Np(2)	3.536(1)	1Ge(1)	3.058(3)
		2Ge(1)	3.089(1)
		4Np(1)	3.536(1)
		4Np(2)	3.833(1)
Central atom: Ge(1)		Central atom: Ge(2)	
Ligand atom	Distance	Ligand atom	Distance
2Np(2)	2.966(3)	6Np(2)	2.848(1)
1Np(2)	3.058(2)	2Ge(2)	2.963(0)
2Np(2)	3.089(2)	6Ge(1)	3.621(3)
4Np(1)	3.136(1)		
2Ge(2)	3.621(3)		
2Ge(1)	3.682(2)		

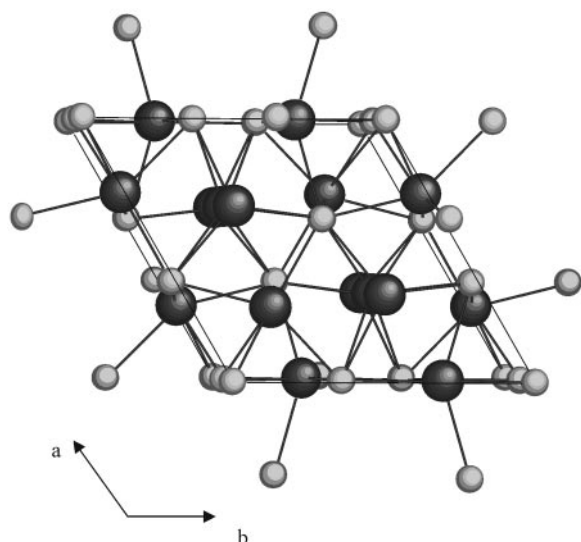


FIG. 5. View of the  $\text{Np}_5\text{Ge}_4$  ( $\text{Ti}_5\text{Ga}_4$  type) crystal structure.

and Ge(3), were obtained. The refinement of the occupation factor of these Ge sites revealed a defect structure only on the Ge(3) site (i.e., the occupation factor drops from 0.125 to 0.048 as the isotropic factor goes from 7.78 to 0.33), leading to the residual values  $R = 0.084$  and  $R_w = 0.109$ . Final refinement including anisotropic displacement parameters led to the conventional residuals factors  $R = 0.071$  and  $R_w = 0.092$ . The positional and the thermal parameters are listed in Table 3. A view of the structure is illustrated in Fig. 3. As mentioned in Ref. (17), this structure is rather complex, due to the great number of different atomic sites. The main feature of this structure is that some Np–Np

interatomic distances are just below the Hill limit where the  $5f$  shells are expected to overlap.

#### $\text{Np}_5\text{Ge}_4$

Figure 4 shows the X-ray powder pattern obtained for the nominal composition  $\text{Np}_5\text{Ge}_4$ . Full profile refinement revealed a hexagonal type unit cell with  $a = 8.8004(9) \text{ \AA}$  and  $c = 5.9274(7) \text{ \AA}$ ,  $c/a = 0.673$ . The structure was successfully refined in the centrosymmetric space group  $P6_3/mcm$ , to the residual values  $R_B = 0.071$  and  $R_F = 0.041$ .  $\text{Np}_5\text{Ge}_4$  crystallizes with the  $\text{Ti}_5\text{Ga}_4$  structure type, as already reported for the homologue uranium binary compounds with Ge(9), Sb(18), and Sn(11). The positional and thermal parameters and the main interatomic distances are listed in Table 4. A view of the crystal structure is displayed in Fig. 5. This structure is characterized by two distinct Np sites. Each Np(1) atom is coordinated by six Ge(1) atoms at  $3.13 \text{ \AA}$  and two other Np(1) atoms with a rather short distance of  $c/2 = 2.96 \text{ \AA}$  leading to straight  $-\text{Np}-\text{Np}-$  infinite chains along the  $c$  axis, whereas Np(2) is surrounded by seven Ge atoms with an average distance of  $2.98 \text{ \AA}$ . Such short distances between Np(1) atoms are smaller than the Hill limit ( $\sim 3.1 \text{ \AA}$ ) and very close to that found in Np metal ( $2.60 \text{ \AA}$  in  $\alpha$ -Np and  $2.76 \text{ \AA}$  in  $\beta$ -Np).

#### $\text{Np}_5\text{Ge}_3$

In the U–Ge binary system, no other compound was observed with a higher content of U than in  $\text{U}_5\text{Ge}_4$  (9). For the Np–Ge system as shown in Fig. 6, we found that Np metal (sg  $Pnma$ ,  $a = 6.685(6) \text{ \AA}$ ,  $b = 4.742(3) \text{ \AA}$ , and

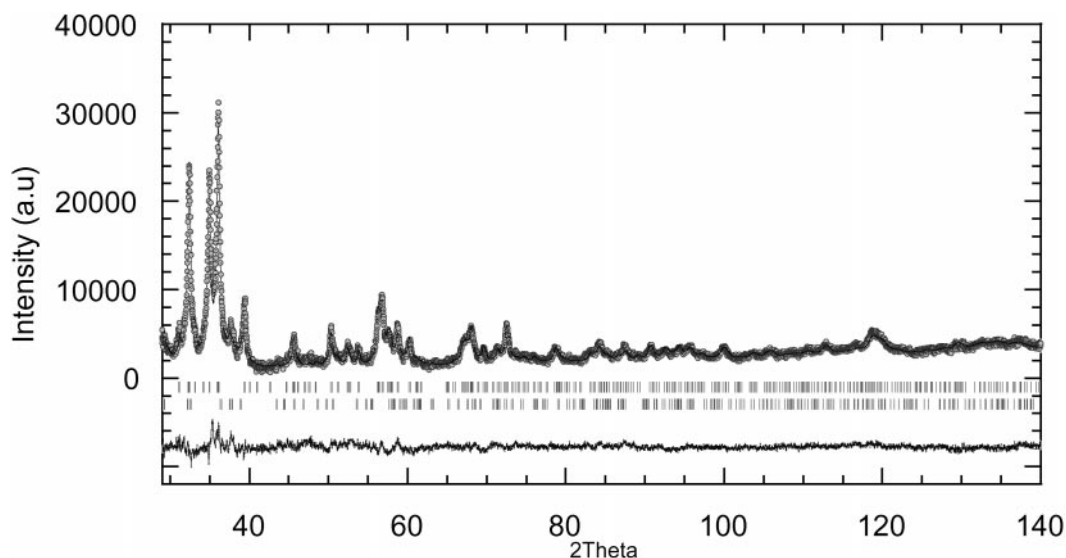


FIG. 6. X-ray powder diffraction pattern of  $\text{Np}_5\text{Ge}_3$  ( $\text{W}_5\text{Si}_3$  type). The symbols represent the observed points; the solid lines represent the calculated profile and the difference between observed and calculated profiles. The ticks correspond to  $2\theta_{hkl}$  Bragg positions (top,  $\text{Np}_5\text{Ge}_3$ ; bottom, Np metal).

**TABLE 5**  
X-Ray Crystallographic Data for  $\text{Np}_5\text{Ge}_3$  ( $\text{W}_5\text{Si}_3$  Type), Atomic Parameters, and Interatomic Distances

Method	sull profile refinement of X-ray powder diffraction data
Space group	$I4/mcm$ , no. 140
Lattice parameters (Å)	$a = 11.434(1)\text{Å}$ , $c = 5.5197(7)\text{Å}$ , $V = 721.6(2)\text{Å}^3$ , $Z = 4$ , $M = 1403.02\text{ g}$
Scan range	$20 < 2\theta < 140$
Number of reflections used in refinement	412
Reliability factors:	
$R_B$	0.071
$R_f$	0.046
$R_p$	0.153
$R_{wp}$	0.183

Atom	Site	Atom parameters			$B$ in $\text{Å}^2$	$\tau_{occ}$
		$x$	$y$	$z$		
Np(1)	4b	0.0	$\frac{1}{2}$	$\frac{1}{4}$	$0.2^a$	1
Np(2)	16k	0.0842(1)	0.2217(1)	0.0	$0.2^a$	1
Ge(1)	4a	0.0	0.0	$\frac{1}{4}$	$0.4^a$	1
Ge(2)	8h	0.1674(5)	$x + \frac{1}{2}$	0.0	$0.4^a$	1

Interatomic distances (in Å)			
Central atom: Np(1)		Central atom: Np(2)	
Ligand atom	distance	Ligand atom	Distance
2Np(1)	2.759(1)	1Ge(2)	2.931(1)
4Ge(2)	2.992(2)	2Ge(1)	3.018(3)
8Np(2)	3.639(1)	1Ge(2)	3.157(2)
		1Np(2)	3.171(1)
		2Ge(2)	3.198(1)
		2Np(2)	3.384(2)
		2Np(2)	3.498(2)
Central atom: Ge(1)		Central atom: Ge(2)	
Ligand atom	Distance	Ligand atom	Distance
2Ge(1)	2.759(1)	2Np(2)	2.931(1)
8Np(2)	3.018(3)	2Np(1)	2.992(2)
8Ge(2)	3.494(3)	2Np(2)	3.157(2)
		4Np(2)	3.198(1)
		2Ge(2)	3.917(2)

<sup>a</sup> Parameters not refined.

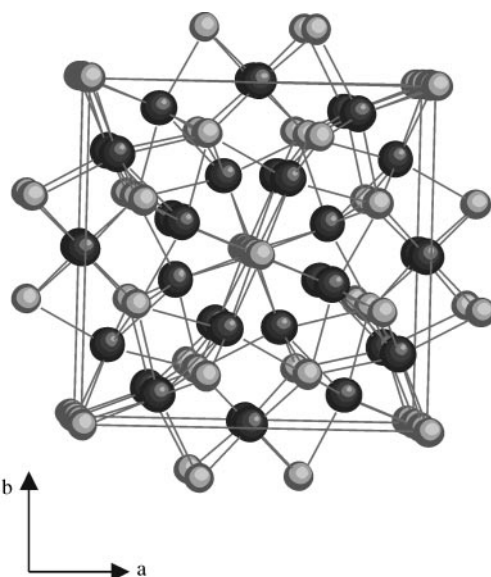


**FIG. 7.** View of the  $\text{Np}_5\text{Ge}_3$  ( $\text{W}_5\text{Si}_3$  type) crystal structure.

$c = 4.920(4)\text{Å}$ ) was not in equilibrium with  $\text{Np}_5\text{Ge}_4$  but with an other phase of the composition,  $\text{Np}_5\text{Ge}_3$ . A look in the literature shows that  $\text{Pu}_5\text{Si}_3$  (19), which crystallizes with the tetragonal  $\text{W}_5\text{Si}_3$ , is the only representative binary actinide already reported with this composition. Analyses of the X-ray powder pattern revealed that  $\text{Np}_5\text{Ge}_3$  crystallizes with a body-centered tetragonal unit cell with  $a = 11.434(1)\text{Å}$  and  $c = 5.5197(7)\text{Å}$ . This phase was refined using the Rietveld method to the  $\text{W}_5\text{Si}_3$  structure type, in the space group  $I4/mcm$ , to the reliability factors of  $R_B = 0.071$  and  $R_f = 0.046$ . The positional and thermal parameters are listed in Table 5. A view of the structure is illustrated in Fig. 7. The  $\text{W}_5\text{Si}_3$  type is also reported to exist in most of the rare earth silicide binary systems, but not with uranium. The striking feature of this structure is that, as observed for  $\text{Np}_5\text{Ge}_4$ , the Np(1) form metallic chains along the  $c$  axis, with interatomic distances equal to  $2.76\text{Å}$ , i.e., much smaller than those observed in  $\text{Np}_5\text{Ge}_4$  and in the same order as in  $\beta\text{-Np}$ .

**TABLE 6**  
Summary of the Crystal Structure of the Binary Silicides and Germanides with Uranium or Neptunium

Structure type/system	AuCu <sub>3</sub>	ZrGa <sub>2</sub>	ThSi <sub>2-x</sub>	AlB <sub>2-x</sub>	USi	ThIn	U <sub>5</sub> Si <sub>4</sub>	Ti <sub>5</sub> Ga <sub>4</sub>	U <sub>3</sub> Si <sub>2</sub>	W <sub>5</sub> Si <sub>3</sub>	AuCu <sub>3</sub> (anti)	Ref.
U–Si	✓	×	✓	✓	✓	×	✓	×	✓	×	✓	[6,20]
Np–Si	✓	?	✓	✓	?	?	?	?	✓	?	?	[21]
U–Ge	✓	✓	✓	✓	×	✓	×	✓	×	×	×	[7–10]
Np–Ge	✓	×	✓	✓	✓	×	×	✓	×	✓	×	this work

Note. (×) Phase does not exist; (✓) phase exists; (?) not investigated.

## CONCLUSION

In this paper we have shown that at least six phases exist in the neptunium–germanium binary system, whereas only one was previously reported in the literature. For comparison, Table 6 gives a summary of the binary silicides and germanides with uranium and neptunium. From pure germanium to the composition NpGe, we observed the structural sequence of AuCu<sub>3</sub>, ThSi<sub>2</sub>, AlB<sub>2</sub>, and USi types, showing more similarities to the U–Si binary system than to the U–Ge system. For the neptunium-rich part, we observed the Ti<sub>5</sub>Ga<sub>4</sub> type, which is also observed in the U–Ge system but not in the U–Si system, and a new type of structure, namely, Np<sub>5</sub>Ge<sub>3</sub> (W<sub>5</sub>Si<sub>3</sub> type) not yet reported in Th or U binary systems. In any case, the study of the physical properties of the new phases isolated is of great interest, especially the influence of the metalloid on the magnetism of neptunium.

## ACKNOWLEDGMENTS

The high-purity Np metal required for the fabrication of the compounds studied here was made available through a loan agreement between Lawrence Livermore National Laboratory and ITU, in the frame of a collaboration involving LLNL, Los Alamos National Laboratory, and the U.S. Department of Energy. P. Boulet acknowledges the European Commission for support given in the frame of the program “Training and Mobility of Researchers.”

## REFERENCES

1. A. Szytula, in “Handbook of Magnetic Materials” (K. H. J. Buschow, Ed.), Vol. 6, p. 85. Elsevier, Amsterdam, 1991.
2. L. C. J. Pereira, F. Wastin, J. M. Winand, B. Kanellakopoulos, J. Rebizant, J. C. Spirlet, and M. Almeida, *J. Solid State Chem.* **134**, 138 (1997).
3. F. Mirambet, P. Gravereau, B. Chevalier, L. Trut, and J. Etourneau, *J. Alloys Compounds* **191**, L1 (1993).
4. T. Le Bihan, H. Noël, K. Hiebl, and P. Rogl, *J. Alloys Compounds* **232**, 142 (1996).
5. F. Wastin, J. Rebizant, J. P. Sanchez, A. Blaise, J. Goffart, J. C. Spirlet, C. T. Walker, and J. Fuger, *J. Alloys Compounds* **210**, 83 (1994).
6. K. Remschnig, T. Le Bihan, H. Noël, and P. Rogl, *J. Solid State Chem.* **97**, 391 (1992).
7. P. Boulet, A. Daoudi, M. Potel, H. Noël, G. M. Gross, G. André, and F. Bourrée, *J. Alloys Compounds* **247**, 104 (1997).
8. P. Boulet, A. Daoudi, M. Potel, and H. Noël, *J. Solid State Chem.* **129**, 113 (1997).
9. P. Boulet, M. Potel, J. C. Levet, and H. Noël, *J. Alloys Compounds* **262/263**, 229 (1997).
10. P. Boulet, M. Potel, G. André, P. Rogl, and H. Noël, *J. Alloys Compounds* **283**, 41 (1999).
11. P. Boulet and H. Noël, *Solid State Commun.* **107**(3), 135 (1998).
12. J. Rodriguez-Carvajal, *Physica B* **192**, 55 (1993).
13. C. K. Fair, “Molen Users Manual. An Interactive Intelligent System for Crystal Structure Analysis.” Delft, The Netherlands, 1989.
14. G. Kimmel, Dept. of Mater. Eng., Israel Inst. of Technology, Technion Haifa, Israel, ICDD Grant-in-Aid, 1993.
15. J. Gal, Z. Hadari, E. R. Bauminger, I. Nowik, and S. Ofer, *Solid State Commun.* **13**, 647 (1973).
16. G. Venturini, I. Ijjaali, and B. Malaman, *J. Alloys Compounds* **285**, 194 (1999).
17. T. Le Bihan, H. Noël, and P. Rogl, *J. Alloys Compounds* **240**, 128 (1996).
18. J. A. Paixao, J. Rebizant, A. Blaise, A. Delapalme, J. P. Sanchez, G. H. Lander, H. Nakotte, P. Burlet, and M. Bonnet, *Physica B* **203**, 137 (1994).
19. D. T. Cromer, A. C. Larson, and R. B. Roof, *Acta Crystallogr.* **17**, 947 (1964).
20. H. Noël, V. Queneau, J. P. Durand, and P. Colomb, in “Abstracts of Int. Conf. on Strongly Correlated Electron Systems-SCES98, 15–18 July, Paris, 1998,” p. 92.
21. P. Villars and L. D. Calvert, “Pearson’s Handbook of Crystallographic Data for Intermetallic Phases.” ASM, Materials Park, OH, 1991.